

the film will no longer be uniform or equi-biaxial. There is a strong orientation to the stress in the vicinity of the steps, with an associated maximum principal compressive stress direction at each point. The wave pattern develops with crests aligned perpendicular to the direction of maximum compressive stress.

The non-uniform pre-buckling stress around steps is derived from a model that approximates the influence of the substrate on the thin film as an attached elastic foundation of springs exerting only tangential forces. The PDMS offers little resistance to displacement of the film in the direction perpendicular to the step; this displacement relieves the stress in that direction, becoming zero at the step itself. A solution for the stresses on either side of an infinitely long isolated step coincident with the y -axis (Fig. 4a) gives equations (4a) and (4b), where σ_x is the stress in the x -direction, σ_y is the stress in the y -direction, and x is measured starting from the step. The transition length l (m) characterizing the distribution of stress from the step to the remote smooth film is given by equation (5).

$$\sigma_x = -\sigma_0[1 - e^{-|x|/l}] \quad (4a)$$

$$\sigma_y = -\sigma_0[1 - \nu_m e^{-|x|/l}] \quad (4b)$$

$$l \approx 0.3t \left[\frac{E_m(1 - \nu_p^2)}{E_p(1 - \nu_m^2)} \right] \approx 0.3t \left[\frac{E_m}{E_p} \right] \approx 1,060t \quad (5)$$

The transition length is 17 times the buckle wavelength, L , for the gold/PDMS system.

The predictability of the wave patterns is demonstrated by analysis of an array of long straight strips parallel to the y -axis, width $2d$, separated by $2D$ (Fig. 4b). The stress distribution in the film before buckling is given by equations (6a) and (6b), for ($|x| < d$) where x is measured from the centre of the strip (Fig. 4c).

$$\sigma_x = -\sigma_0 \left[1 - \frac{\cosh(x/l)}{\cosh(d/l)} \right] \quad (6a)$$

$$\sigma_y = -\sigma_0 \left[1 - \nu_m \frac{\cosh(x/l)}{\cosh(d/l)} \right] \quad (6b)$$

The stresses between the strips are given by the same formulae, but with d replaced by D , and with x now measured from the centre of that region. We note that the compressive stress in the y -direction remains relatively large, with a minimum, $-\sigma_0(1 - \nu_m)$ at the step; the compressive stress in the x -direction is smaller everywhere, and zero at the step. Consistent with σ_y being larger than σ_x , the wave pattern shows crests aligned perpendicular to the y -axis (Fig. 4d).

The process described here provides a remarkable example of the spontaneous generation of complexity. The regularity in the waves reflects the uniformity in the physical properties and dimensions of the materials. The ability to control the orientation and periodicity of these waves by changing these parameters, and by patterning the surface of the PDMS using straightforward techniques, makes this system eminently controllable. We believe that this process offers potential to generate planar and non-planar surfaces patterned in 1–100 μm features over many square centimetres. Such patterns are interesting for their potential applications in sensors and optical components (for example, diffraction gratings): they also allow mapping of material properties in two dimensions. Most interestingly, such patterns offer the opportunity to study the generation of complex ordered structure from simple patterns. \square

Received 7 January; accepted 16 March 1998.

- Whitesides, G. M., Mathias, J. P. & Seto, C. T. Molecular self-assembly and nanochemistry: a chemical strategy for the synthesis of nanostructures. *Science* **254**, 1312–1319 (1991).
- Desiraju, G. R. *Crystal Engineering: The Design of Organic Solids* (Elsevier, New York, 1989).
- van Blaaderen, A., Ruel, R. & Wiltzius, P. Template-directed colloidal crystallization. *Nature* **385**, 321–324 (1997).
- Bain, C. D. *et al.* Formation of monolayer films by the spontaneous assembly of organic thiols from solution onto gold. *J. Am. Chem. Soc.* **111**, 321–335 (1989).
- Voet, D. & Voet, J. G. *Biochemistry* (Wiley, New York, 1995).

- Davis, M. E., Lobo, R. F. Zeolite and molecular sieve synthesis. *Chem. Mater.* **4**, 756–768 (1992).
- Lewis, D. W., Willock, D. J., Catlow, C. R. A., Thomas, J. M. & Hutchings, G. J. De novo design of structure-directing agents for the synthesis of microporous solids. *Nature* **382**, 604–606 (1996).
- Makse, H. A., Havlin, S., King, P. R. & Stanley, H. E. Spontaneous stratification in granular mixtures. *Nature* **386**, 379–382 (1997).
- Jaeger, H. M. & Nagel, S. R. Physics of the granular state. *Science* **255**, 1523–1531 (1992).
- Zik, O., Levine, D., Shtrikman, S. G. & Stavans, J. Rotationally induced segregation of granular materials. *Phys. Rev. Lett.* **73**, 644–647 (1994).
- Knight, J. B., Jaeger, H. M. & Nagel, S. R. Vibration-induced size separation in granular media: the convection connection. *Phys. Rev. Lett.* **70**, 3728–3731 (1993).
- Bodo, P. & Sundgren, J.-E. Titanium deposition onto ion-bombarded and plasma-treated polydimethylsiloxane: surface modification, interface, and adhesion. *Thin Solid Films* **136**, 147–159 (1986).
- Martin, G. C. *et al.* The metallization of silicone polymers in the rubbery and the glassy state. *J. Appl. Phys.* **53**, 797–799 (1982).
- Allen, H. G. *Analysis and Design of Structural Sandwich Panels* (Pergamon, New York, 1969).
- Hutchinson, J. W., Thouless, M. D. & Liniger, E. G. Growth and configuration stability of circular, buckling-driven film delaminations. *Acta Metall. Mater.* **40**, 295–308 (1992).
- Kumar, A., Abbott, N. L., Kim, E., Biebuyck, H. A. & Whitesides, G. M. Patterned self-assembled monolayers and meso-scale phenomena. *Acc. Chem. Res.* **28**, 219–226 (1995).
- Xia, Y. & Whitesides, G. M. Soft Lithography. *Angew. Chem. Int. Edn* **37**, 550–575 (1998).
- Ohring, M. *The Material Science of Thin Films* (Academic, San Diego, 1992).

Acknowledgements. We thank D. Munn for helpful discussions. This work was supported by the NSF, the Office of Naval Research, and the Defense Advanced Research Projects Agency. N.B. thanks the Department of Defense for a predoctoral fellowship.

Correspondence and requests for materials should be addressed to G.M.W. (e-mail: gwhitesides@gmgroup.harvard.edu).

Polymer gels with engineered environmentally responsive surface patterns

Zhibing Hu*, Yuanye Chen*, Changjie Wang*, Yindong Zheng* & Yong Li†

* Department of Physics, University of North Texas, Denton, Texas 76203, USA

† Kimberly-Clark Corporation, Neenah, Wisconsin 54956, USA

The polymer gels called hydrogels may be induced to swell or shrink (taking up or expelling water between the crosslinked polymer chains) in response to a variety of environmental stimuli, such as changes in pH or temperature, or the presence of a specific chemical substrate¹. These gels are being explored for several technological applications, particularly as biomedical materials². When hydrogels swell or shrink, complex patterns may be generated on their surfaces^{3–7}. Here we report the synthesis and controlled modulation of engineered surface patterns on environmentally responsive hydrogels. We modify the character of a gel surface by selectively depositing another material using a mask. For example, we use sputter deposition to imprint the surface of an *N*-isopropylacrylamide (NIPA) gel with a square array of gold thin films. The periodicity of the array can be continuously varied as a function of temperature or electric field (which alter the gel's volume), and so such an array might serve as an optical grating for sensor applications. We also deposit small areas of an NIPA gel on the surface of an acrylamide gel; the patterned area can be rendered invisible reversibly by switching the temperature above or below the lower critical solution temperature of the NIPA gel. We anticipate that these surface patterning techniques may find applications in display and sensor technology.

We first discuss the surface patterns made by use of the sputtering-deposition technique. *N*-isopropylacrylamide (NIPA) gel slabs were made by free-radical polymerization, as follows. A mixture of 7.8 g of *N*-isopropylacrylamide, 133 mg of methylene-bis-acrylamide as a crosslinker, and tetramethylethylenediamine (240 μl) as an accelerator, was dissolved in 100 ml of deionized and distilled water. Nitrogen gas was bubbled through the solution to remove dissolved oxygen. The polymerization was initiated by adding 40 mg of ammonium persulphate. The samples were kept in water for several days to wash out chemical residues. The NIPA gels were then

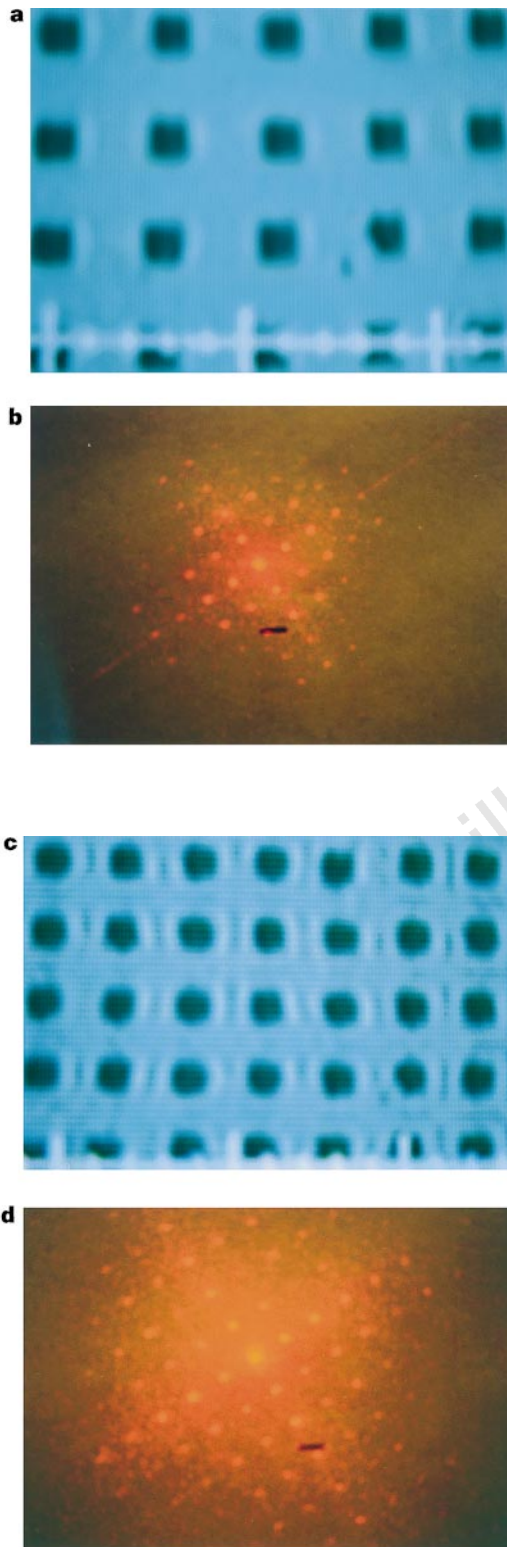


Figure 1 The periodic square surface array on the NIPA hydrogel and its diffraction pattern, at various temperatures. At 30°C: **a**, the surface array; **b**, the diffraction pattern. At 33.6°C: **c**, the surface array; **d**, the diffraction pattern. In the diffraction experiment, the distance between the screen and the sample was 95 cm. In **a** and **c**, each small division in the white scale at the bottom of the image is 0.0193 mm; in **b** and **d**, the black bar is 1 cm long.

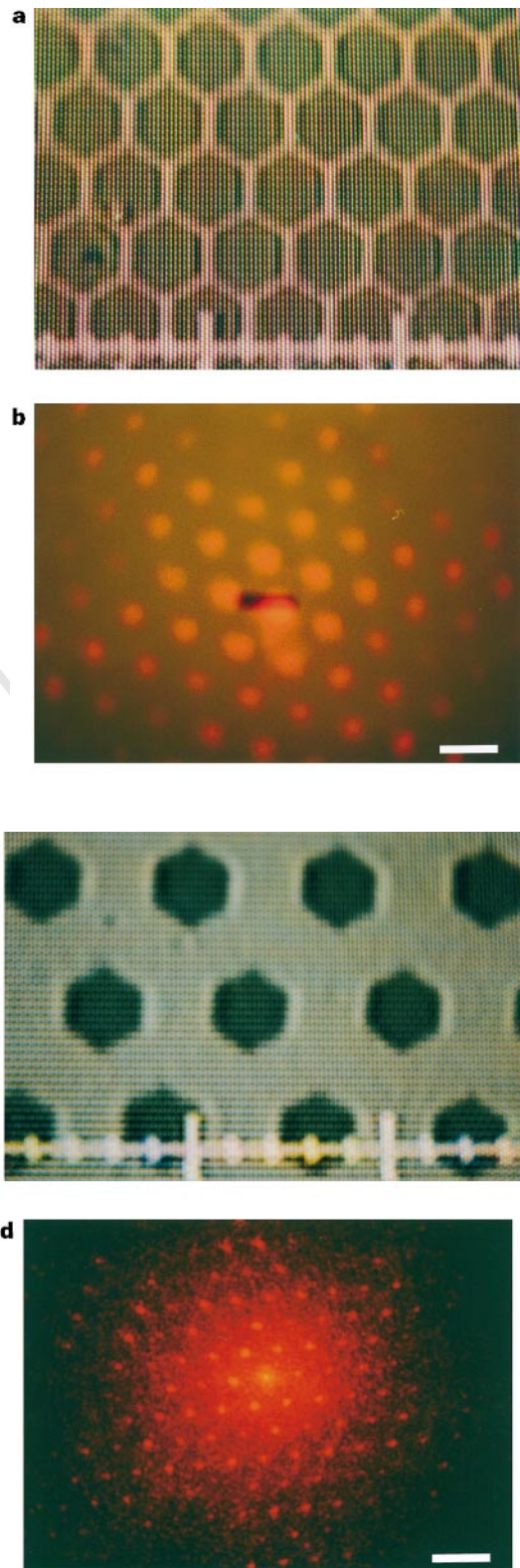


Figure 2 The periodic hexagonal surface array on the NIPA gel in the dehydrated and in the hydrated states at room temperature. **a**, The surface array of a dry NIPA gel film. **b**, The light diffraction pattern produced by the sample in **a**. **c**, The increased periodicity of the surface structure after immersion of the dry gel in water. **d**, The corresponding diffraction pattern from the sample of **c**. In the diffraction experiment, the distance between the screen and the sample was 100 cm. In **a** and **c**, each small division in the white scale at the bottom of the image is 0.0193 mm; in **b** and **d** the white bar is 2 cm long.

dried slowly in a partially sealed glass container so that they shrank uniformly.

SPI Slim Bar Grids (SPI supplies, West Chester, Pennsylvania) were used as masks for the sputter deposition. For the square mesh grid, the bar width was 6 μm and the hole width was 19 μm . A dry NIPA gel was covered by a grid and placed on the anode in the chamber of a sputter coater. During the coating operation, the chamber was pumped to a low-level vacuum with an argon gas pressure of 0.04 mbar. A sputtering voltage of 2.5 kV was applied to ionize the argon. When the argon ions struck the gold cathode, gold atoms were ejected and impinged upon the sample through the openings of the mask. This process was continued for ~ 3.5 min, giving a gold thickness of ~ 53 nm. After coating, the mask was removed and the gel was immersed in water. The affinity between gold and the polymer gel may be due to the interaction between the lone-pair electron of the amine group in the NIPA gel and the empty orbitals of gold⁸, and to entrapment of gold in the gel. The temperature of samples was controlled by a circulation water bath. The sample surfaces were examined by an optical microscope, and the diffraction experiment was performed by placing the gel sample between a He-Ne laser and a screen. The microscopic structure and the diffraction patterns were recorded using a camera.

Figure 1a shows the surface array of a swollen NIPA gel film in water at 30 $^{\circ}\text{C}$. The dark area is the gold-covered surface and the light area is the bare gel surface. The spaces between the small gold squares in the gel surface can serve as slits for light diffraction. Because such slits are aligned in both the x - and y -directions, the

diffraction pattern should consist of bright and dark spots instead of fringes when monochromatic light passes through these slits. Such a diffraction pattern is shown in Fig. 1b.

As the temperature was increased from room temperature, the NIPA gel shrank owing to the volume phase transition⁴. This caused the array periodic constant (d) to decrease. The periodic surface array and its diffraction pattern for the gel at 33.6 $^{\circ}\text{C}$ are shown in Fig. 1c and d, respectively. The gel was thermally cycled at least seven times, and the temperature-induced change in the diffraction pattern was observed to be reversible. Several different samples were synthesized and tested, and their diffraction patterns were also reproducible. We have also successfully 'tuned' the periodicity of the surface array of an ionic NIPA gel by applying an electric field. The electric field caused migration of positive counter ions and water inside the gel towards the negative electrode, and resulted in volume shrinkage⁹.

Although the surface arrays discussed here have a periodic square structure, many other structural arrays may be synthesized by using different masks; these include strip, rectangular, hexagonal, and even non-periodic surface arrays. Figure 2a shows a hexagonal surface array on a dehydrated NIPA gel at room temperature. The corresponding diffraction pattern is shown in Fig. 2b and exhibits a clear six-fold symmetry. When the gel is fully swollen in water at room temperature, the periodicity of the surface array is significantly larger, as is clearly demonstrated by both optical (Fig. 2c) and diffraction (Fig. 2d) observations.

The periodic array produced on the gel surface can serve as a two-dimensional grating, and may be compared with a previous study of three-dimensional diffraction from a crystalline colloidal array of polystyrene spheres embedded within a gel¹⁰. The width of the slits and the number of the slits per unit area of the gel surface grating can be changed by external stimuli such as temperature and electric field. The location of the diffraction bright spots is described by $\sin\theta_x = n\lambda/d_x$ and $\sin\theta_y = m\lambda/d_y$; here subscripts x and y represent the horizontal and the vertical direction, respectively, θ is the angle relative to the central spot, λ is the wavelength (633 nm for the He-Ne laser), n and m are the order of diffraction, and d is the grating constant or periodicity. As the periodicity of the gel surface pattern changes in response to the external stimuli, the diffraction angle should change accordingly. Such a gel grating has potential for applications in optical filters and sensors, and in optical communications.

The gel with periodic surface patterns can be used as a sensor. For example, the deformation of a gel under external force can be easily monitored using such a gel. In one experiment, we suspended in water a gel with a periodic surface array, and subjected it to a uniaxial force at its bottom end along the y -direction. Diffraction patterns of the gel were recorded for various loads. For zero force, the separation (Δl_x) between neighbouring diffraction spots along the x -direction was equal to that (Δl_y) along the y -direction. The ratio of $\Delta l_y/\Delta l_x$ decreased, however, as the external force increased. For the load of 5.85 g, $\Delta l_y/\Delta l_x \approx 0.72$.

This incorporation of a metal array on a hydrogel surface opens a new avenue to the manufacture of microelectrode array devices which can greatly enhance sensor performance¹¹. The combination of microelectrode arrays and 'smart' gels has potential applications in ion chromatography¹¹, the detection of enzyme activity¹², and the monitoring of cell electrical activity¹³.

We now consider the synthesis of an engineered surface pattern; this was accomplished by depositing one polymer gel (NIPA) on the surface of another polymer gel (polyacrylamide, PAAM, gel). The PAAM gel was made using the NIPA recipe but with 7.8 g of *N*-isopropylacrylamide replaced by 5 g of acrylamide, the use of 13.3 mg rather than 40 mg of ammonium persulphate, and the addition of 4 mg riboflavin-5'-phosphate (ultraviolet photoinitiator). The NIPA pre-gel solution was put on the surface of the PAAM gel; the sample was then covered by a mask (we used an outline map

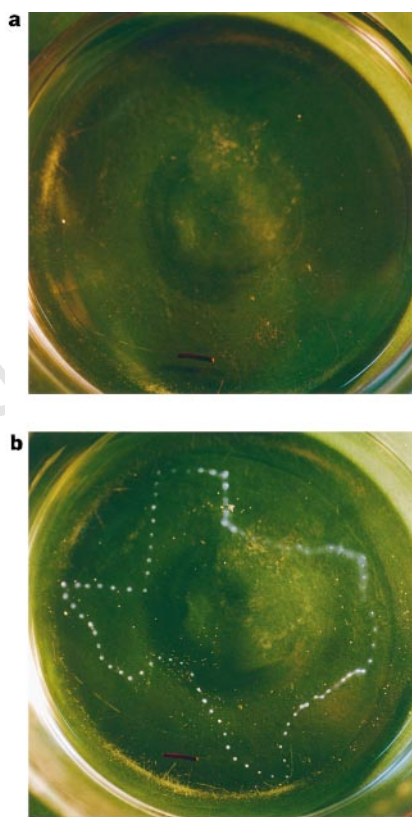


Figure 3 Temperature-responsive surface pattern in the NIPA-deposited PAAM gel. **a**, At room temperature, the NIPA-deposited PAAM gel is transparent and no surface pattern is seen. **b**, When heated to above 37 $^{\circ}\text{C}$, the outline image of Texas appears. This is because at $>37^{\circ}\text{C}$ the polymerized NIPA-deposited areas become cloudy while the PAAM gel remains transparent. The whole process takes ~ 10 s, and after the sample is cooled down, the map disappears: the process is fully reversible. Scale bar, 1 cm.

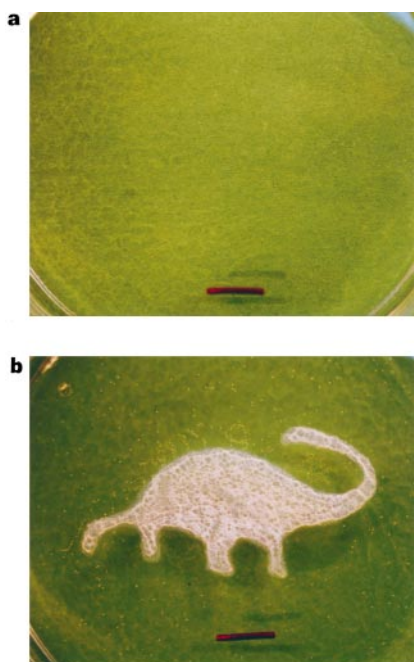


Figure 4 A gel display with a solid image. **a**, At room temperature, the NIPA-deposited PAAM gel is transparent and no surface pattern is seen. **b**, When heated to $>37^{\circ}\text{C}$, the solid image of a dinosaur appears. Scale bar, 1 cm.

of Texas) and illuminated by ultraviolet light for ~ 60 min. The NIPA solution gelled only at areas that were exposed to ultraviolet light; at these areas, an interpenetrating polymer network¹⁴ of NIPA and PAAM was formed, with an estimated depth of ~ 0.5 mm.

As both the PAAM substrate and the NIPA gel on the surface of the substrate are transparent at room temperature, no surface structure can be observed (Fig. 3a). When this surface-engineered sample was warmed up to 37°C , the areas of polymerized NIPA become cloudy^{15,16} while the PAAM gel remained in the transparent state. As a result, the outline image of a Texas map appears at the surface of the PAAM gel (Fig. 3b). This map can be turned on or turned off by simply 'switching' the temperature above or below the lower critical solution temperature, T_c ($= 34^{\circ}\text{C}$) of the NIPA gel. The switching time was ~ 10 s, much shorter than that required for a shape memory gel¹⁴.

To further demonstrate the potential of the gels with engineered surface patterns, a gel display consisting of a PAAM substrate with the NIPA gel filling the unmasked surface area was made, and is shown immersed in water in Fig. 4. At room temperature (Fig. 4a), both NIPA and PAAM gels were transparent and no pattern was observed. At 37°C (Fig. 4b), the NIPA-deposited area becomes cloudy, and results in appearance of a solid image; a representation of a dinosaur. The gel display developed here is responsive to temperature, but by changing the chemical composition of the gels, the gel displays could be made responsive to other external stimuli such as salt concentration and infrared light. The image of the gel display can be clearly seen at any angle, in contrast to a well established liquid-crystal display that requires head-on viewing angles. □

Received 20 November 1997; accepted 24 February 1998.

1. Tanaka, T. Gels. *Sci. Am.* **244**, 124–138 (1981).
2. Peppas, N. A. & Langer, R. New challenges in biomaterials. *Science* **263**, 1715–1720 (1994).
3. Tanaka, T. *et al.* Mechanical instability of gels at the phase transition. *Nature* **325**, 796–798 (1987).
4. Sato-Matsuo, E. & Tanaka, T. Patterns in shrinking gels. *Nature* **358**, 482–485 (1992).
5. Li, Y., Li, C. & Hu, Z. Pattern formation of constrained acrylamide/sodium acrylate copolymer gels in acetone/water mixture. *J. Chem. Phys.* **100**, 4637–4644 (1994).
6. Li, C., Hu, Z. & Li, Y. Temperature and time dependence of patterns of surface patterns in constrained ionic N-isopropylacrylamide gels. *J. Chem. Phys.* **100**, 4645–4652 (1994).

7. Suzuki, A., Yamazaki, M. & Kobiki, Y. Direct observation of polymer gel surfaces by atomic force microscopy. *J. Chem. Phys.* **104**, 1751–1757 (1996).
8. Grabar, K. C., Freeman, G. G., Hommer, M. B. & Natan, M. J. Preparation and characterization of Au colloid monolayers. *Anal. Chem.* **67**, 735–743 (1995).
9. Hirotsu, S. Electric-field-induced phase transition in polymer gels. *Jpn J. Appl. Phys.* **24**, 396–398 (1985).
10. Weissman, J. M., Sunkara, H. B., Tse, A. S. & Asher, S. A. Thermally switchable periodicities and diffraction from mesoscopically ordered materials. *Science* **274**, 959–960 (1996).
11. Imisides, M. D., John, R. & Wallace, G. G. Microsensors based on conducting polymers. *Chemtech* **26**, 19–25 (1996).
12. Wang, J. & Chen, Q. Enzyme microelectrode array strips for glucose and lactate. *Anal. Chem.* **66**, 1007–1011 (1994).
13. Misch, W., Bock, J., Egert, U., Hammerle, H. & Mohr, A. A thin film microelectrode array for monitoring extracellular neuronal activity in vitro. *Biosensors Bioelectr.* **9**, 737–741 (1994).
14. Hu, Z., Zhang, X. & Li, Y. Synthesis and application of modulated polymer gels. *Science* **269**, 525–527 (1995).
15. Li, Y., Wang, G. & Hu, Z. Turbidity study of spinodal decomposition of N-isopropylacrylamide gels. *Macromolecules* **28**, 4194–4197 (1995).
16. Bansil, R., Liao, G. & Falus, P. Kinetics of spinodal decomposition in chemically crosslinked gels. *Physica A* **231**, 346–358 (1996).

Acknowledgements. We thank the Donors of the Petroleum Research Fund, administered by the American Chemical Society, and the US Army Research Office for support of this work.

Host-guest encapsulation of materials by assembled virus protein cages

Trevor Douglas* & Mark Young†

* Department of Chemistry, Temple University, Philadelphia, Pennsylvania 19122-2585, USA

† Department of Plant Pathology, Montana State University, Bozeman, Montana 59717-0314, USA

Self-assembled cage structures of nanometre dimensions can be used as constrained environments for the preparation of nanostructured materials^{1,2} and the encapsulation of guest molecules³, with potential applications in drug delivery⁴ and catalysis⁵. In synthetic systems the number of subunits contributing to cage structures is typically rather small^{3,6}. But the protein coats of viruses (virions) commonly comprise hundreds of subunits that self-assemble into a cage for transporting viral nucleic acids. Many virions, moreover, can undergo reversible structural changes that open or close gated pores to allow switchable access to their interior⁷. Here we show that such a virion—that of the cowpea chlorotic mottle virus—can be used as a host for the synthesis of materials. We report the mineralization of two polyoxometalate species (paratungstate and decavanadate) and the encapsulation of an anionic polymer inside this virion, controlled by pH-dependent gating of the virion's pores. The diversity in size and shape of such virus particles make this a versatile strategy for materials synthesis and molecular entrapment.

We have used the well defined cowpea chlorotic mottle virus (CCMV)⁷ as a model system for reversibly gated entrapment of inorganic minerals and an organic polymer. CCMV virions are 280 Å in diameter and the protein shell defines an inner cavity ~ 180 Å in diameter as measured by electron microscopy. This virus is composed of 180 identical coat protein subunits arranged on an icosahedral lattice. Purified viral coat protein subunits can be easily assembled *in vitro* into empty virion particles⁸. The dimensions of the virion cavity define the upper limit for crystal growth of the entrapped mineral. In addition, each coat protein subunit presents at least nine basic residues (arginine and lysine) to the interior of the cavity⁹. This creates a positively charged interior cavity surface, which provides an interface for inorganic crystal nucleation and growth. From the structure of the CCMV particle it is known that the outer surface of the protein shell is not highly charged⁷, thus the inner and outer surfaces of this molecular container provide chemically unique environments which we have exploited to spatially localize and control the mineralization reaction.